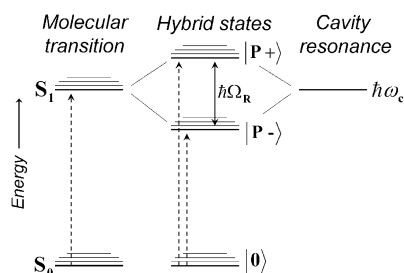


# Modifying Chemical Landscapes by Coupling to Vacuum Fields\*\*

James A. Hutchison, Tal Schwartz, Cyriaque Genet, Eloïse Devaux, and Thomas W. Ebbesen\*

Just as atoms exchange electrons to form molecular orbitals, an electromagnetic field can interact with a quantum system by the exchange of photons. When this interaction is strong enough to overcome decoherence effects, new hybrid light–matter states can form, separated by what is known as the Rabi splitting energy (Figure 1). This strong coupling regime



**Figure 1.** Simplified energy landscape showing the interaction of a HOMO–LUMO ( $S_0$ – $S_1$ ) transition of a molecule resonant with a cavity mode  $\hbar\omega_c$ . When energy exchange between the molecular transition and the cavity is rapid compared to energy loss, strong coupling leads to the formation of two hybrid light–matter (polaritonic) states  $|P+\rangle$  and  $|P-\rangle$ , separated by the Rabi splitting energy  $\hbar\Omega_R$ . Note that the absolute energy of the ground level of the coupled system  $|0\rangle$  may also be modified by strong coupling.

is typically achieved by placing the material in an optical cavity, such as that formed by two parallel mirrors, which is tuned to be resonant with a transition to an excited state. Theory, discussed below, shows that even in the absence of light, a residual splitting always exists due to coupling to vacuum (electromagnetic) fields in the cavity. While cavity strong coupling and the associated hybrid states have been extensively studied due to the potential they offer in physics such as room temperature Bose–Einstein condensates and thresholdless lasers,<sup>[1–14]</sup> the implication for chemistry remains totally unexplored. This is despite the fact that strong coupling with organic molecules lead to exceptionally large vacuum Rabi splittings (hundreds of meV) due to their large transition dipole moments.<sup>[15–24]</sup> The molecules plus the cavity must thus be thought of as a single entity with new energy levels and therefore should have its own distinct chemistry.

We demonstrate here that one can indeed influence a chemical reaction by strongly coupling the energy landscape governing the reaction pathway to vacuum fields.

In the absence of dissipation, the Rabi splitting energy  $\hbar\Omega_R$  (Figure 1) between the two new hybrid light–matter states is given, for a two-level system at resonance with a cavity mode, by the product of the electric field amplitude  $E$  in the cavity and the transition dipole moment  $d$ :<sup>[13]</sup>

$$\hbar\Omega_R = 2Ed\sqrt{n_{\text{ph}} + 1} = 2\sqrt{\frac{\hbar\omega}{2\varepsilon_0 V}}d\sqrt{n_{\text{ph}} + 1} \quad (1)$$

where  $\hbar\omega$  is the cavity resonance or transition energy,  $\varepsilon_0$  the vacuum permittivity,  $V$  the mode volume and  $n_{\text{ph}}$  the number of photons in the cavity. As can be seen, even when  $n_{\text{ph}}$  goes to zero, there remains a finite value for the Rabi splitting,  $\hbar\Omega_{\text{VRS}}$ , due to the interaction with the vacuum field. This splitting is itself proportional to the square root of the number of molecules in the cavity  $\sqrt{n_{\text{mol}}}$ <sup>[13,14]</sup> which in turn implies that  $\hbar\Omega_{\text{VRS}}$  is proportional to the square root of the concentration  $\sqrt{n_{\text{mol}}/V}$ , as observed experimentally for instance in the case of molecules strongly coupled with surface plasmons.<sup>[21]</sup>

We chose as a model system a photochrome which provides one form with a transition dipole moment  $d$  to favor strong coupling [Eq. (1)] and the associated chemical reaction is monomolecular to avoid any complications due to diffusion. The photochromic molecule is the spirocyanine (SPI) derivative 1',3'-dihydro-1',3',3'-trimethyl-6-nitrospiro[2H-1-benzopyran-2,2'-(2H)-indole] which undergoes ring cleavage following photoexcitation to form a merocyanine (MC) (Figure 2a). The extended conjugation of the latter results in strong absorption in the visible (Figure 2c, red curve). The reverse reaction can be achieved photochemically or by thermal means. The simplified potential energy surface for this photochrome is shown schematically in Figure 2b. The absorption spectrum of the SPI form in a poly(methylmethacrylate) (PMMA) film is shown in Figure 2c. Upon irradiation at 330 nm, the SPI photoisomerizes to the MC form and the absorbance of the MC form ( $\lambda_{\text{max}} = 560$  nm, red curve Figure 2c) increases until the photostationary state is reached.

To form the resonant cavity, the PMMA film containing the photochrome was sandwiched between two Ag mirrors, insulated from direct contact to the Ag by thin poly(vinyl alcohol) (PVA) films as shown in Figure 2d. The first Ag mirror was deposited on the glass substrate but note that the second mirror was not sputtered nor evaporated directly on the PMMA film to avoid any possible perturbation of the chemical system. Instead the top Ag film was deposited on a separate block of poly(dimethylsiloxane) (PDMS) which was then transferred to the sample, effectively encapsulating the photochrome in the microcavity (see Supporting Information

[\*] Dr. J. A. Hutchison,<sup>[†]</sup> Dr. T. Schwartz,<sup>[†]</sup> Dr. C. Genet, Dr. E. Devaux, Prof. T. W. Ebbesen  
ISIS, Université de Strasbourg and CNRS (UMR 7006)  
Strasbourg (France)  
E-mail: ebbesen@unistra.fr

[†] These authors contributed equally to this work.

[\*\*] This research was supported by the ERC (grant no. 227577).

Supporting information for this article is available on the WWW under <http://dx.doi.org/10.1002/anie.201107033>.

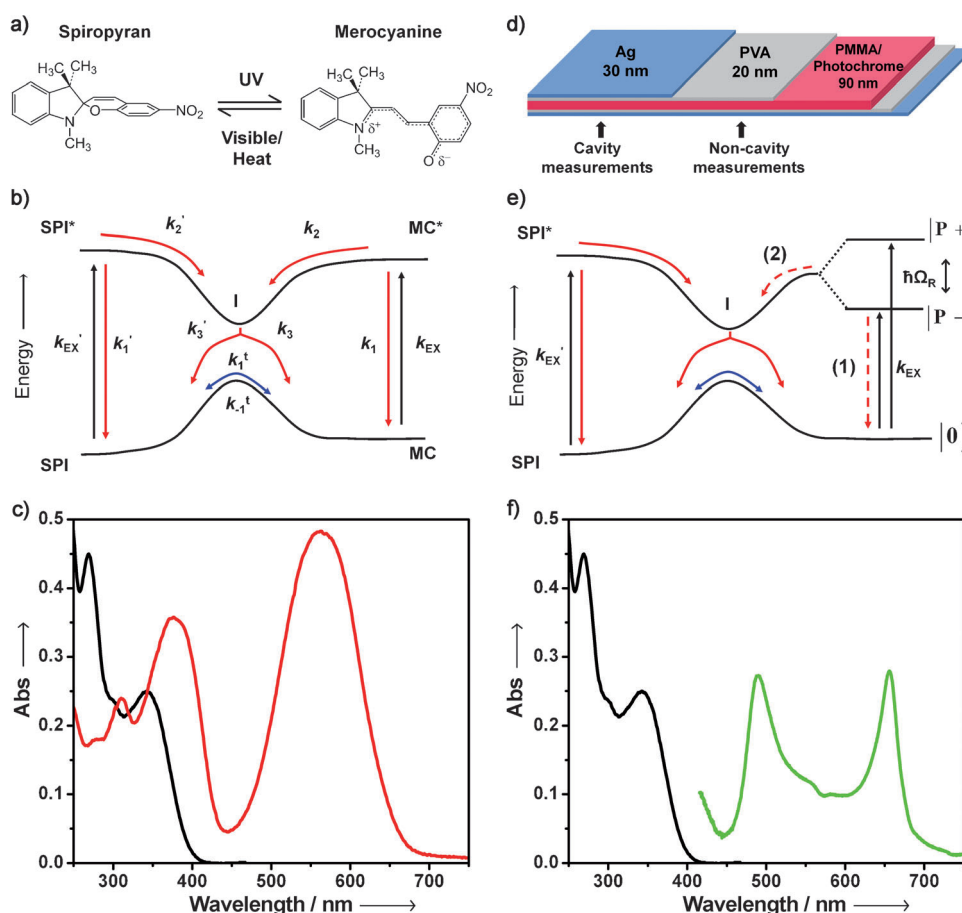


**Figure 2.** a) The molecular structure of spiropyran (SPI) and merocyanine (MC). b) Diagram of the energy landscape connecting the two isomers in the ground and first excited state where  $k_{\text{EX}}$  and  $k_{\text{EX}}'$  are the rates of photoexcitation and the others the rates of the internal pathways; for example,  $k_1$  represents the sum of non-radiative and radiative relaxation rates from  $\text{MC}^*$  to MC. Vibrational sub-levels are not included for clarity. c) The ground state absorption spectra of SPI (black) and MC (red) in PMMA film. d) The structure of the cavity; note that cavity and non-coupled measurements were done concurrently on the same film. e) Diagram of the energy landscape connecting the two isomers in the ground and first excited state, with modification of the MC states by strong coupling and the appearance of the polariton states  $|P+\rangle$  and  $|P-\rangle$ , separated by the Rabi splitting  $\hbar\Omega_R$ . f) The ground state absorption spectra of SPI (black) in PMMA and of the coupled system (green, structure shown in (d)) determined experimentally in the available wavelength window by measuring the transmission  $T$  and reflection  $R$  of the sample ( $\text{Abs} = 1 - T - R$ ).

for details). The transmission spectrum of this cavity structure is characterized by two features: a peak at 326 nm due to the transparency window of silver corresponding to its plasma frequency, and the fundamental Fabry–Perot cavity mode, which for a total PVA/PMMA/PVA thickness of 130 nm occurs at 560 nm (these cavity transmission features can be seen in Figure 3 a, black curve).<sup>[24]</sup> The Fabry–Perot mode is therefore resonant with the absorption of MC. UV irradiation of the cavity at 330 nm causes formation of MC just as for the case of the isolated PMMA film.

When the MC is strongly coupled to the vacuum field in the cavity, the resulting formation of the hybrid states (or polaritons) is evidenced by the splitting of the absorption into two new peaks (green curve Figure 2 f). The detailed physics of the strong coupling of this particular system have been presented elsewhere.<sup>[24]</sup> In brief, at the photostationary state, ca. 80% of the MC species are strongly coupled and the

vacuum Rabi splitting is in the order of 700 meV (Figure 2 f). In other words, the new hybrid states,  $|P+\rangle$  and  $|P-\rangle$ , have absorptions at  $\pm 350$  meV relative to the transition energy of the uncoupled MC (2.2 eV). Note that this Rabi splitting does not arise from the photons used to probe the system but is only due to the vacuum field as can be seen from the fact that the spectrum of the coupled molecules is independent of the weak light intensity used to record it.

We now analyze the photoisomerization kinetics inside and outside the cavity. The detailed photoisomerization mechanism, schematically simplified in Figure 2b, is still in debate in the literature due to its complexity and is reported to involve several intermediate isomers, including the triplet manifold, here collectively shown as a single species I.<sup>[25–29]</sup> Nevertheless the reaction proceeds with observed first-order kinetics in solution. An overall first-order reaction mechanism ( $k_{\text{obs}}$ ) is also predicted from the simplified reaction diagram in Figure 2b where  $k_{\text{obs}}$  is a complex function of the quantum yields of the various individual photoinduced steps:

$$\frac{d[\text{MC}]}{dt} = -k_{\text{obs}}[\text{MC}] + b$$

$$\text{with } k_{\text{obs}} = \left( \frac{k_3'}{k_3 + k_3'} \frac{k_2}{k_1 + k_2} + \frac{k_3}{k_3 + k_3'} \frac{k_2'}{k_1' + k_2'} \right) k_{\text{ex}} \quad (2)$$

$$\text{and } b = \frac{k_3}{k_3 + k_3'} \frac{k_2'}{k_1' + k_2'} k_{\text{ex}} [\text{SPI}]_0$$

The detailed derivation of this rate equation is given in the Supporting Information. It assumes that the intermediates  $\text{SPI}^*$ , I and  $\text{MC}^*$  are in a stationary state and it is simplified by irradiation at the isosbestic point for the two species at 330 nm. The photostationary (PS) concentration ratio under the experimental conditions for this model is given by:

$$\frac{[\text{MC}]_{\text{PS}}}{[\text{SPI}]_{\text{PS}}} = \frac{k_3 k_2'}{k_3' (k_1 + k_2')} \left( 1 + \frac{k_1}{k_2} \right) \quad (3)$$

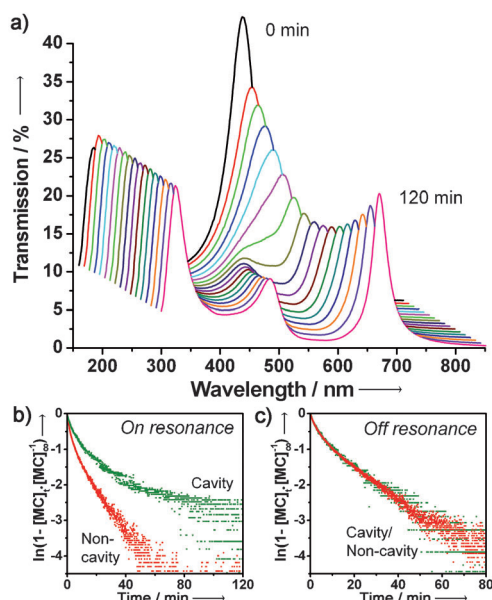


**Figure 3.** a) Transmission spectrum of the coupled system in the cavity as a function of irradiation time at 330 nm where the Ag film has a transparency window as seen in the spectra. Notice that the initial Fabry–Perot mode at ca. 560 nm (black curve) splits into two new modes as the SPI to MC photoreaction proceeds. b) Kinetics of the growth of the MC absorbance (i.e. concentration) measured for the bare molecules (red) and the coupled system (green) in the configuration shown in Figure 2 d; in other words, the uncoupled molecules were irradiated through one mirror on the same sample as the cavity system involving two mirrors. The negative log plot stems from taking  $\ln(1 - [MC]_t/[MC]_\infty)$  versus  $t$ . For this case, in which the cavity resonance is tuned to exactly match the MC absorption at 560 nm, the difference in the rates increases with the degree of strong coupling. c) In contrast, when the cavity thickness is tuned such that it is non-resonant with the MC absorption for all angles of incidence, the photoisomerization rate is identical to that of the non-cavity sample.

In a polymer matrix, the internal isomerization processes are further complicated by convolution with the heterogeneous segmental motion of the polymer resulting in deviations from exponential behavior.<sup>[29]</sup> The kinetic build-up of MC in the PMMA matrix (outside the cavity) during UV irradiation at 330 nm shows indeed deviation from linearity when plotted on a log scale (red points in Figure 3b). Shown in Figure 3a is the progression of the same reaction, but inside the cavity, monitored by transmission spectra of the cavity structure. The Fabry–Perot mode is reduced and splits as the MC concentration increases. Using transfer matrix simulations, the transmission spectra as a function of time allow us to calculate the absorbance of MC at each time. This data is superimposed on that of the bare molecular film in Figure 3b, making a slight correction for the different intensities of 330 nm light impinging on the polymer layer for the open structure and for the cavity (around 20% higher in the latter case). It is clear (Figure 3b) that while the rates measured for the two systems are similar at early times, as the reaction proceeds, the observed photoisomerization rate is slowed down significantly in the cavity structure. This retardation corresponds to the onset of strong-coupling conditions and

the formation of the hybrid light–matter states. The larger the splitting, the slower is the overall reaction reaching a fraction of the initial rate. We stress that the intensity of the UV light penetrating the cavity remains constant, which is ensured by the invariance of the spectrum around 330 nm. Hence, the change in rate cannot be attributed to a simple optical effect. The final concentrations of the species at the photostationary state are also modified, increasing the MC yield in the cavity by ca. 10%. Furthermore, it was checked that when the cavity is designed in such a way to be out of resonance (at all angles) with the MC absorption transition, there is no change in rate (Figure 3c) compared to the film outside the cavity.

A slowing of SPI-MC photoisomerization as the system enters strong-coupling conditions is fully consistent with the change in energy landscape in Figure 2e and Equation (2). The upper lying  $|P+\rangle$  state will rapidly decay to  $|P-\rangle$  which in turn by lying lower than the uncoupled excited state  $MC^*$  will favor the return to ground state (path (1) over path (2) in Figure 2e). The corresponding change in the rate constants  $k_1$  and  $k_2$  would result in a reduction in  $k_{obs}$  for the photoisomerization (through the decrease of the  $k_2/(k_1+k_2)$  term in Equation (2)) and an increase in the photostationary concentration of coupled MC [ $k_1/k_2$  increases in Eq. (3)], as is observed.

While the modification of the reaction potential by strong coupling shown in Figure 1 and 2 emphasizes the splitting of the excited-state energy levels, one must bear in mind that this modification will be “felt” through the entire system, reordering the energy levels including possibly the ground state. If that is the case, the formation of the light–matter hybrid state might not only alter the photoisomerization rates between SPI and MC, but also the thermal conversion of MC to SPI in the ground-state energy landscape. Theoretical considerations of such ultra-strong coupling regime (into which this cavity/photochrome system falls)<sup>[24]</sup> also predict a modification of the ground-state energy.<sup>[11,12]</sup> Nevertheless, careful analysis of the thermal back reaction did not reveal any change in the rate beyond experimental error.

To gain further insight into the photochemical events, transient differential absorption spectroscopy (pump–probe) experiments were carried out on the coupled system and compared to that of the uncoupled molecules. This technique has the advantage of probing the excited states by detecting very small absorbance changes with minimal perturbation of the system, with the ability to also detect non-radiative decay processes in contrast to time-resolved fluorescence. Figure 4a shows the transient spectra immediately after the 150 fs pump pulse (560 nm) for different coupling strengths. As can be seen, the transient spectra are all very different from that of the uncoupled molecules. To understand these spectra, it is worth remembering that the transient differential absorption  $\Delta A(\lambda)$  is given by Equation (4):<sup>[30]</sup>

$$\Delta A(\lambda) = [\sigma^*(\lambda) - \sigma_0(\lambda) - \sigma_{SE}(\lambda)] \kappa d [MC^*] \quad (4)$$

where  $\sigma^*(\lambda)$  is the excited-state absorption cross-section in  $\text{cm}^{-2}$ ,  $\sigma_0(\lambda)$  the ground-state absorption cross-section,  $\sigma_{SE}(\lambda)$  the stimulated-emission cross-section of the excited state,  $\kappa$  the constant that relates the molar extinction coefficient to

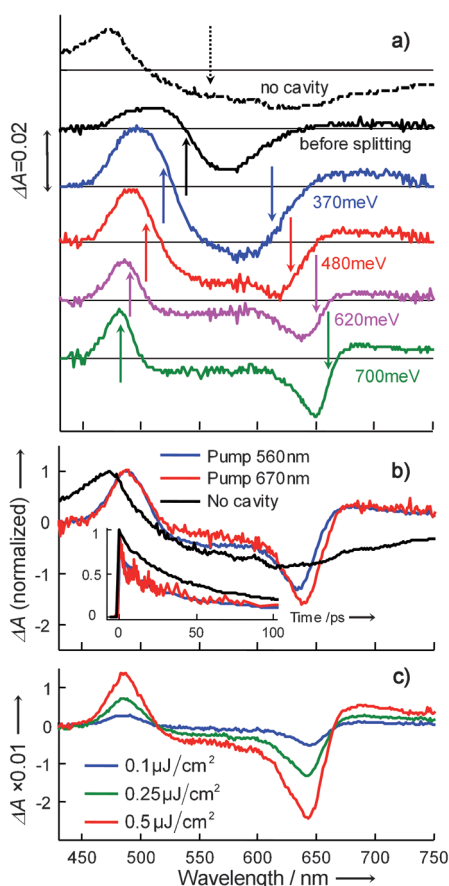


**Figure 4.** Transient spectra and kinetics of the coupled system. a) Transient spectra recorded immediately after the 150-fs pump pulse at 560 nm for a bare molecular film and the cavity system for different coupling strengths. The arrows mark the position of the bare molecule absorption peak (topmost curve), and the linear transmission peaks of the cavity for each coupling strength. Note that the apparent bleaching at the absorption wavelengths of the lower polariton just reflects the fact that its absorption cross-section to higher excited states is lower than that of the ground state to  $|P-\rangle$  while the reverse is true at the wavelengths where upper polariton absorbs [Eq. (3)]. b) Transient spectra at the maximum coupling strength recorded after excitation at different wavelengths as indicated. Inset: decay kinetics at the same wavelengths compared to the absence of cavity. c) Transient spectra at different excitation intensities.

the cross-section ( $2.63 \times 10^{20} \text{ M}^{-1} \text{ cm}$ ) and  $d$  (cm) the path-length or thickness of the film.

The spectra contain both positive peaks where the transient state absorbs more than the ground state and negative peaks at wavelengths where either the second and/or third term in Equation (4) dominate(s). The contribution of these terms to the spectra of the coupled system depends on the coupling strength in two ways. As the vacuum Rabi splitting increases, the photophysical properties of the coupled system are gradually modified but at the same time the fraction of coupled molecules increases. In other words, in such disordered molecular systems both coupled (polariton) and non-coupled (incoherent) states coexist,<sup>[6,7]</sup> and both are excited by the pump pulse and thereby contribute to the transient spectrum. At the strongest coupling strength, the transient absorption spectrum is dominated by the coupled

system. This can be checked by changing the excitation to wavelengths where the coupled system absorbs more strongly as shown in Figure 4b. By exciting at 670 nm directly in the ground state to  $|P-\rangle$  absorption band, the transient spectrum is only slightly modified. This also indicates that the recorded transient spectrum for the coupled system is essentially the differential absorption between  $|P-\rangle$  and ground state. In other words, the  $|P+\rangle$  state is too short-lived to be detected in the 150 fs resolution of the apparatus. It is common in molecules that the lower excited state is the longest lived. That is why fluorescence is typically observed only from  $|P-\rangle$ , if at all.<sup>[17]</sup> Finally, it was also checked that the shape of the transient spectrum is invariant with the pump intensity and that the differential absorbance increases linearly (Figure 4c), demonstrating thereby that the signal is due to a mono-photon transition to the excited state. It also confirms that the Rabi splitting is a result of coupling to the vacuum field.

The uncoupled (bare) molecules display a small amount of stimulated emission in the transient experiments and they also undergo spontaneous fluorescence from the lowest excited state, typical of aromatic organic molecules. The strongly coupled system showed no emission (spontaneous or stimulated) indicating again significant changes in the photo-physical dynamics. The kinetics of the transient spectra are also modified by the strong coupling (inset, Figure 4b). The decay kinetics of the excited uncoupled MC is not a single exponential in agreement with other fs studies<sup>[27]</sup> and as discussed earlier it is due to the involvement of several intermediate isomers and matrix heterogeneity. The first half-life is ca. 30 ps while that of the coupled system is shortened to 10 ps (inset, Figure 4b). This reduction in  $|P-\rangle$  lifetime inside the cavity is totally consistent with the results of the steady-state irradiation experiments as discussed above.<sup>[31]</sup>

The rearrangement of the molecular energy levels by coupling to the vacuum field has numerous important consequences for molecular and material sciences. As we have shown here, it can be used to modify chemical energy landscapes and in turn the reaction rates and yields. Strong coupling can either speed up or slow down a reaction depending on the reorganization of specific energy levels relative to the overall energy landscape. Both rates and the thermodynamics of the reaction will be modified. It is important not to confuse reaction modification by strong coupling in the vacuum field regime with such phenomena as photochemical reactions in strong fields where the molecules retain their electronic structure and the rates are enhanced by concentrating the light. Although the semi-classical approach can be used to predict the shape of the spectrum and the Rabi splitting in strongly coupled systems, it cannot account for the lifetime of the discrete states, their dynamics and their interrelationships. For this the quantum nature of the field needs to be invoked.

The coupling was done here to an electronic transition but it could also be done to a specific vibrational transition for instance to modify the reactivity of a bond. In this way it can be seen as analogous to a catalyst which changes the reaction rate by modifying the energy landscape. Like all chemical reactions, the effect is favored by higher concentrations but for a different reason—here it modifies the energy landscape

and not just simply the collision rates. Since the formation of hybrid states changes the energy levels at play, it will in principle modify the ionization potential and the electron affinity of the system. So not only will the redox reactions be affected, but we also expect that the work function of the coupled material will be modified and measurements to verify this are underway. Fine tuning the work function by strong coupling to vacuum fields could have significant consequences for device design and performance, for instance in the case of organic light emitting diodes, photovoltaics and molecular electronics. It is important to note that in the context of applications, strong coupling is not limited to the Fabry–Perot configuration used here. Any photonic structure that provides a sufficiently sharp resonance can be used. When using molecular materials with large transition dipole moments, even low-quality resonators are sufficient to generate strong coupling, especially when the mode-volume is small such as in the case of a metallic microcavity or a confined surface plasmon resonance generated on metallic hole arrays.<sup>[15–24]</sup> Such “open” plasmonic structures can be accessed more easily for further characterization and for connection to more complex functionalities.

The harvesting of cavity vacuum fields for modifying chemical reaction landscapes and material properties puts an entirely new tool into the hands of the chemist for influencing useful reactions, with important implications for material science and molecular devices. It is thus an area of much scientific and technological potential and warrants further exploration.

Received: October 5, 2011  
Revised: November 18, 2011  
Published online: January 10, 2012

**Keywords:** cavity quantum electrodynamics · energy landscape · hybrid light–matter states · strong coupling · vacuum field

- [1] D. Snoke, P. Littlewood, *Phys. Today* **2010**, *63*, 42–47.
- [2] J. M. Raimond, M. Brune, S. Haroche, *Rev. Mod. Phys.* **2001**, *73*, 565–582.
- [3] M. S. Skolnick, T. A. Fisher, D. M. Whittaker, *Semicond. Sci. Technol.* **1998**, *13*, 645–669.
- [4] C. Weisbuch, M. Nishioka, A. Ishikawa, Y. Arakawa, *Phys. Rev. Lett.* **1992**, *69*, 3314–3317.
- [5] V. Savona, L. C. Andreani, P. Schwendimann, A. Quattropani, *Solid State Commun.* **1995**, *93*, 733–739.
- [6] V. M. Agranovitch, M. Litinskaia, D. G. Lidzey, *Phys. Rev. B* **2003**, *67*, 085311.
- [7] M. Litinskaya, P. Reineker, V. M. Agranovich, *J. Lumin.* **2004**, *110*, 364–372.
- [8] J. P. Reithmaier, G. Sęk, A. Löffler, C. Hofmann, S. Kuhn, S. Reitzenstein, L. V. Keldysh, V. D. Kulakovskii, T. L. Reinecke, A. Forchel, *Nature* **2004**, *432*, 197–200.

- [9] T. Yoshie, A. Scherer, J. Hendrickson, G. Khitrova, H. M. Gibbs, G. Rupper, C. Ell, O. B. Shchekin, D. G. Deppe, *Nature* **2004**, *432*, 200–203.
- [10] G. Zumofen, N. M. Mojarad, V. Sandoghdar, M. Agio, *Phys. Rev. Lett.* **2008**, *101*, 180404.
- [11] C. Ciuti, G. Bastard, I. Carusotto, *Phys. Rev. B* **2005**, *72*, 115303.
- [12] A. A. Anappara, S. De Liberato, A. Tredicucci, C. Ciuti, G. Biasiol, L. Sorba, F. Beltram, *Phys. Rev. B* **2009**, *79*, 201303(R).
- [13] S. Haroche, D. Kleppner, *Phys. Today* **1989**, *42*, 24–30.
- [14] R. J. Thompson, G. Rempe, H. J. Kimble, *Phys. Rev. Lett.* **1992**, *68*, 1132–1135.
- [15] D. G. Lidzey, D. D. C. Bradley, M. S. Skolnick, T. Virgili, S. Walker, D. M. Whittaker, *Nature* **1998**, *395*, 53–55.
- [16] P. A. Hobson, W. L. Barnes, D. G. Lidzey, G. A. Gehring, D. M. Whittaker, M. S. Skolnick, *Appl. Phys. Lett.* **2002**, *81*, 3519–3521.
- [17] J. Bellessa, C. Bonnand, J. C. Plenet, J. Mugnier, *Phys. Rev. Lett.* **2004**, *93*, 036404.
- [18] R. J. Holmes, S. R. Forrest, *Phys. Rev. Lett.* **2004**, *93*, 186404.
- [19] F. Sasaki, S. Haraichi, S. Kobayashi, *J. Quantum Electron.* **2002**, *38*, 943–948.
- [20] J. R. Tischler, M. S. Bradley, V. Bulović, J. H. Song, A. Nurmikko, *Phys. Rev. Lett.* **2005**, *95*, 036401.
- [21] J. Dintinger, S. Klein, F. Bustos, W. L. Barnes, T. W. Ebbesen, *Phys. Rev. B* **2005**, *71*, 035424.
- [22] A. Salomon, C. Genet, T. W. Ebbesen, *Angew. Chem.* **2009**, *121*, 8904–8907; *Angew. Chem. Int. Ed.* **2009**, *48*, 8748–8751.
- [23] T. K. Hakala, J. J. Toppari, A. Kuzyk, M. Pettersson, H. Tikkänen, H. Kunttu, P. Törmä, *Phys. Rev. Lett.* **2009**, *103*, 053602.
- [24] T. Schwartz, J. A. Hutchison, C. Genet, T. W. Ebbesen, *Phys. Rev. Lett.* **2011**, *106*, 196405.
- [25] C. Lenoble, R. S. Becker, *J. Phys. Chem.* **1986**, *90*, 62–65.
- [26] A. K. Chibisov, H. Görner, *J. Phys. Chem. A* **1997**, *101*, 4305–4312.
- [27] J. Hopley, U. Pfeifer-Fukumura, M. Bletz, T. Asahi, H. Masuhara, H. Fukumura, *J. Phys. Chem. A* **2002**, *106*, 2265–2270.
- [28] C. J. Wohl, D. Kuciauskas, *J. Phys. Chem. B* **2005**, *109*, 22186–22191.
- [29] G. Such, R. A. Evans, L. H. Yee, T. P. Davis, *J. Macromol. Sci. C: Polym. Rev.* **2003**, *43*, 547–579.
- [30] M. Becker, V. Nagarajan, W. W. Parson, *J. Am. Chem. Soc.* **1991**, *113*, 6840–6848.
- [31] Perhaps the more surprising is why the lifetime of |P−) is not roughly that of the lifetime of the photon in the cavity, that is, very short on the order of tens of fs. From the width of the Fabry–Perot resonance, the damping time in the cavity is ca. 25 fs. The lifetime of the MC\* is much longer, on the order of tens of ps, so one would expect that the lifetime of the polaritonic state would be dominated by the shorter of the two since it is formed by a coherent photon exchange between the molecule and the cavity. One explanation for the observed longer lifetime of polaritonic states involving molecules has been explained by energy transfer from incoherent uncoupled molecules to the coherent polaritonic states.<sup>[6,7]</sup> If this was the case here, then the transient absorption spectrum would be that of the uncoupled molecules which it is clearly not (Figure 4). Another explanation must therefore be sought to explain such results.